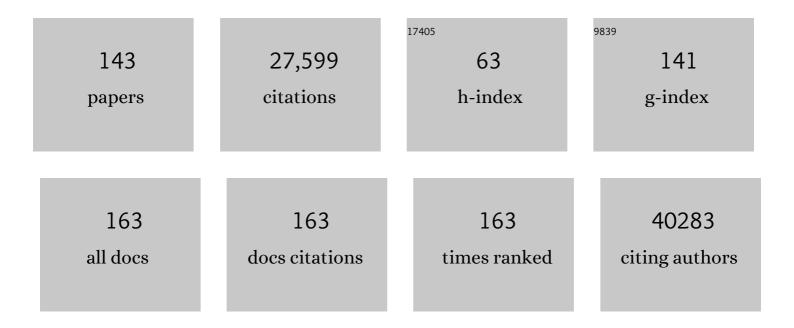
## **Urs Schaltegger**

List of Publications by Year in descending order

Source: https://exaly.com/author-pdf/9290534/publications.pdf Version: 2024-02-01



#	Article	IF	CITATIONS
1	The driving mechanisms of the carbon cycle perturbations in the late Pliensbachian (Early Jurassic). Scientific Reports, 2019, 9, 18430.	1.6	9,028
2	Plešovice zircon — A new natural reference material for U–Pb and Hf isotopic microanalysis. Chemical Geology, 2008, 249, 1-35.	1.4	3,858
3	The Composition of Zircon and Igneous and Metamorphic Petrogenesis. Reviews in Mineralogy and Geochemistry, 2003, 53, 27-62.	2.2	3,181
4	Re-equilibration of Zircon in Aqueous Fluids and Melts. Elements, 2007, 3, 43-50.	0.5	661
5	Growth, annealing and recrystallization of zircon and preservation of monazite in high-grade metamorphism: conventional and in-situ U-Pb isotope, cathodoluminescence and microchemical evidence. Contributions To Mineralogy and Petrology, 1999, 134, 186-201.	1.2	600
6	Correlating the end-Triassic mass extinction and flood basalt volcanism at the 100 ka level. Geology, 2010, 38, 387-390.	2.0	372
7	Timing of the Early Triassic carbon cycle perturbations inferred from new U–Pb ages and ammonoid biochronozones. Earth and Planetary Science Letters, 2007, 258, 593-604.	1.8	237
8	Tracking the evolution of large-volume silicic magma reservoirs from assembly to supereruption. Geology, 2013, 41, 867-870.	2.0	226
9	The Bushveld Complex was emplaced and cooled in less than one million years – results of zirconology, and geotectonic implications. Earth and Planetary Science Letters, 2015, 418, 103-114.	1.8	218
10	Magmatic-to-hydrothermal crystallization in the W–Sn mineralized Mole Granite (NSW, Australia). Chemical Geology, 2005, 220, 191-213.	1.4	215
11	How Accurately Can We Date the Duration of Magmatic-Hydrothermal Events in Porphyry Systems?An Invited Paper. Economic Geology, 2013, 108, 565-584.	1.8	213
12	New Early to Middle Triassic U–Pb ages from South China: Calibration with ammonoid biochronozones and implications for the timing of the Triassic biotic recovery. Earth and Planetary Science Letters, 2006, 243, 463-475.	1.8	212
13	End-Triassic mass extinction started by intrusive CAMP activity. Nature Communications, 2017, 8, 15596.	5.8	211
14	U-Pb geochronologic evidence for the evolution of the Gondwanan margin of the north-central Andes. Bulletin of the Geological Society of America, 2007, 119, 697-711.	1.6	204
15	Incremental growth of the Patagonian Torres del Paine laccolith over 90 k.y. Geology, 2008, 36, 459.	2.0	204
16	Pre-Mesozoic Alpine basements—Their place in the European Paleozoic framework. Bulletin of the Geological Society of America, 2013, 125, 89-108.	1.6	204
17	U–Th–Pb zircon geochronology by ID-TIMS, SIMS, and laser ablation ICP-MS: Recipes, interpretations, and opportunities. Chemical Geology, 2015, 402, 89-110.	1.4	204
18	Uî—,Pb age constraints on deposition and provenance of Birimian and gold-bearing Tarkwaian sediments in Ghana, West Africa. Precambrian Research, 1994, 67, 89-107.	1.2	190

#	Article	IF	CITATIONS
19	Zircon and titanite recording 1.5 million years of magma accretion, crystallization and initial cooling in a composite pluton (southern Adamello batholith, northern Italy). Earth and Planetary Science Letters, 2009, 286, 208-218.	1.8	175
20	Refertilization of mantle peridotite in embryonic ocean basins: trace element and Nd isotopic evidence and implications for crust–mantle relationships. Earth and Planetary Science Letters, 2004, 221, 293-308.	1.8	174
21	Rates of magma differentiation and emplacement in a ballooning pluton recorded by U–Pb TIMS-TEA, Adamello batholith, Italy. Earth and Planetary Science Letters, 2012, 355-356, 162-173.	1.8	173
22	Precise U–Pb age constraints for end-Triassic mass extinction, its correlation to volcanism and Hettangian post-extinction recovery. Earth and Planetary Science Letters, 2008, 267, 266-275.	1.8	166
23	Crustal-scale magmatic systems during intracontinental strike-slip tectonics: U, Pb and Hf isotopic constraints from Permian magmatic rocks of the Southern Alps. International Journal of Earth Sciences, 2007, 96, 1131-1151.	0.9	156
24	Towards accurate numerical calibration of the Late Triassic: High-precision U-Pb geochronology constraints on the duration of the Rhaetian. Geology, 2014, 42, 571-574.	2.0	154
25	High temperature (>350°C) thermochronology and mechanisms of Pb loss in apatite. Geochimica Et Cosmochimica Acta, 2014, 127, 39-56.	1.6	154
26	Evaluating the temporal link between the Karoo LIP and climatic–biologic events of the Toarcian Stage with high-precision U–Pb geochronology. Earth and Planetary Science Letters, 2014, 408, 48-56.	1.8	145
27	Hydrothermal Zircon. Elements, 2007, 3, 51-79.	0.5	133
28	New highâ€resolution age data from the Ediacaran–Cambrian boundary indicate rapid, ecologically driven onset of the Cambrian explosion. Terra Nova, 2019, 31, 49-58.	0.9	131
29	Evolution of the Adria-Europe plate boundary in the northern Dinarides: From continent-continent collision to back-arc extension. Tectonics, 2010, 29, n/a-n/a.	1.3	125
30	Detrital zircon fingerprint of the Proto-Andes: Evidence for a Neoproterozoic active margin?. Precambrian Research, 2008, 167, 186-200.	1.2	123
31	Tectonomagmatic evolution of Western Amazonia: Geochemical characterization and zircon U-Pb geochronologic constraints from the Peruvian Eastern Cordilleran granitoids. Bulletin of the Geological Society of America, 2009, 121, 1298-1324.	1.6	122
32	The transition from rifting to sea-floor spreading within a magma-poor rifted margin: field and isotopic constraints. Terra Nova, 2002, 14, 156-162.	0.9	121
33	Multiple mantle sources during island arc magmatism: U-Pb and Hf isotopic evidence from the Kohistan arc complex, Pakistan. Terra Nova, 2002, 14, 461-468.	0.9	118
34	U–Pb zircon and monazite geochronology of Variscan magmatism related to syn-convergence extension in Central Northern Portugal. Lithos, 2005, 82, 169-184.	0.6	118
35	Time resolved construction of a bimodal laccolith (Torres del Paine, Patagonia). Earth and Planetary Science Letters, 2012, 325-326, 85-92.	1.8	116
36	Age and isotopic constraints on magmatism along the Karakoram-Kohistan Suture Zone, NW Pakistan: evidence for subduction and continued convergence after India-Asia collision. Swiss Journal of Geosciences, 2007, 100, 85-107.	0.5	108

#	Article	IF	CITATIONS
37	Rapid heterogeneous assembly of multiple magma reservoirs prior to Yellowstone supereruptions. Scientific Reports, 2015, 5, 14026.	1.6	100
38	The age and source of late Hercynian magmatism in the central Alps: evidence from precise U?Pb ages and initial Hf isotopes. Contributions To Mineralogy and Petrology, 1992, 111, 329-344.	1.2	99
39	Crustal growth along a non-collisional cratonic margin: A Lu–Hf isotopic survey of the Eastern Cordilleran granitoids of Peru. Earth and Planetary Science Letters, 2009, 279, 303-315.	1.8	99
40	No evidence for Hadean continental crust within Earth's oldest evolved rock unit. Nature Geoscience, 2016, 9, 777-780.	5.4	99
41	Linking rapid magma reservoir assembly and eruption trigger mechanisms at evolved Yellowstone-type supervolcanoes. Geology, 2014, 42, 807-810.	2.0	97
42	Magma pulses in the Central Variscan Belt: episodic melt generation and emplacement during lithospheric thinning. Terra Nova, 1997, 9, 242-245.	0.9	96
43	Zircon ages of high-grade gneisses in the Eastern Erzgebirge (Central European) Tj ETQq1 1 0.784314 rgBT /Ove Variscan foldbelt. Lithos, 2001, 56, 303-332.	rlock 10 Ti 0.6	f 50 507 Td ( 94
44	A new method integrating high-precision U–Pb geochronology with zircon trace element analysis (U–Pb TIMS-TEA). Geochimica Et Cosmochimica Acta, 2010, 74, 7144-7159.	1.6	92
45	Characterisation of Triassic rifting in Peru and implications for the early disassembly of western Pangaea. Gondwana Research, 2016, 35, 124-143.	3.0	92
46	Rapid burial and exhumation during orogeny: Thickening and synconvergent exhumation of thermally weakened and thinned crust (Variscan orogen in Western Europe). Numerische Mathematik, 2002, 302, 856-879.	0.7	89
47	Developing a strategy for accurate definition of a geological boundary through radio-isotopic and biochronological dating: The Early–Middle Triassic boundary (South China). Earth-Science Reviews, 2015, 146, 65-76.	4.0	87
48	What is the tectono-metamorphic evolution of continental break-up: The example of the Tasna Ocean–Continent Transition. Journal of Structural Geology, 2006, 28, 1849-1869.	1.0	85
49	Geochronological constraints on post-extinction recovery of the ammonoids and carbon cycle perturbations during the Early Jurassic. Palaeogeography, Palaeoclimatology, Palaeoecology, 2012, 346-347, 1-11.	1.0	85
50	Post-granulite facies monazite growth and rejuvenation during Permian to Lower Jurassic thermal and fluid events in the Ivrea Zone (Southern Alps). Contributions To Mineralogy and Petrology, 1999, 134, 405-414.	1.2	84
51	Late Cretaceous intra-oceanic magmatism in the internal Dinarides (northern Bosnia and) Tj ETQq1 1 0.784314 n 106-125.	gBT /Over 0.6	lock 10 Tf 50 83
52	The current state and future of accessory mineral research. Chemical Geology, 2002, 191, 3-24.	1.4	82
53	Magmatic-to-hydrothermal crystallization in the W–Sn mineralized Mole Granite (NSW, Australia). Chemical Geology, 2005, 220, 215-235.	1.4	82
54	Lower crustal melting and the role of open-system processes in the genesis of syn-orogenic quartz diorite–granite–leucogranite associations: constraints from Sr–Nd–O isotopes from the Bandombaai Complex, Namibia. Lithos, 2003, 67, 205-226.	0.6	81

#	Article	IF	CITATIONS
55	Zircons reveal magma fluxes in the Earth's crust. Nature, 2014, 511, 457-461.	13.7	81
56	Precise age for the Permian–Triassic boundary in South China from high-precision U-Pb geochronology and Bayesian age–depth modeling. Solid Earth, 2017, 8, 361-378.	1.2	76
57	Precise UPb chronometry of 345-340 Ma old magmatism related to syn-convergence extension in the Southern Vosges (Central Variscan Belt). Earth and Planetary Science Letters, 1996, 144, 403-419.	1.8	74
58	Cenozoic granitoids in the Dinarides of southern Serbia: age of intrusion, isotope geochemistry, exhumation history and significance for the geodynamic evolution of the Balkan Peninsula. International Journal of Earth Sciences, 2011, 100, 1181-1206.	0.9	74
59	Neodymium and strontium isotopic dating of diagenesis and low-grade metamorphism of argillaceous sediments. Geochimica Et Cosmochimica Acta, 1994, 58, 1471-1481.	1.6	73
60	Petrochronology of Zircon and Baddeleyite in Igneous Rocks: Reconstructing Magmatic Processes at High Temporal Resolution. Reviews in Mineralogy and Geochemistry, 2017, 83, 297-328.	2.2	72
61	High-precision dating of the Kalkarindji large igneous province, Australia, and synchrony with the Early–Middle Cambrian (Stage 4–5) extinction. Geology, 2014, 42, 543-546.	2.0	70
62	New constraints on the Jurassic–Cretaceous boundary in the High Andes using high-precision U–Pb data. Gondwana Research, 2014, 26, 374-385.	3.0	67
63	High-resolution insights into episodes of crystallization, hydrothermal alteration and remelting in the Skaergaard intrusive complex. Earth and Planetary Science Letters, 2012, 355-356, 199-212.	1.8	65
64	The data treatment dependent variability of U–Pb zircon ages obtained using mono-collector, sector field, laser ablation ICPMS. Journal of Analytical Atomic Spectrometry, 2012, 27, 663.	1.6	65
65	EOCENE ZIRCON REFERENCE MATERIAL FOR MICROANALYSIS OF U-Th-Pb ISOTOPES AND TRACE ELEMENTS. Canadian Mineralogist, 2014, 52, 409-421.	0.3	65
66	U–Pb, Re–Os, and 40Ar/39Ar geochronology of the Nambija Au-skarn and Pangui porphyry Cu deposits, Ecuador: implications for the Jurassic metallogenic belt of the Northern Andes. Mineralium Deposita, 2009, 44, 371-387.	1.7	64
67	U-Pb geochronology of the Southern Black Forest Batholith (Central Variscan Belt): timing of exhumation and granite emplacement. International Journal of Earth Sciences, 2000, 88, 814-828.	0.9	61
68	Two types of ultrapotassic plutonic rocks in the Bohemian Massif — Coeval intrusions at different crustal levels. Lithos, 2010, 115, 163-176.	0.6	58
69	Syn-convergent high-temperature metamorphism and magmatism in the Variscides: a discussion of potential heat sources. Geological Society Special Publication, 2000, 179, 387-399.	0.8	57
70	Mesozoic arc magmatism along the southern Peruvian margin during Gondwana breakup and dispersal. Lithos, 2012, 146-147, 48-64.	0.6	57
71	Calibrating chemical abrasion: Its effects on zircon crystal structure, chemical composition and U Pb age. Chemical Geology, 2019, 511, 1-10.	1.4	57
72	High-precision zircon U–Pb geochronology of astronomically dated volcanic ash beds from the Mediterranean Miocene. Earth and Planetary Science Letters, 2014, 407, 19-34.	1.8	56

#	Article	IF	CITATIONS
73	Timing of juvenile arc crust formation and evolution in the Sapat Complex (Kohistan–Pakistan). Chemical Geology, 2011, 280, 243-256.	1.4	55
74	Timing of incremental pluton construction and magmatic activity in a back-arc setting revealed by ID-TIMS U/Pb and Hf isotopes on complex zircon grains. Chemical Geology, 2013, 342, 76-93.	1.4	54
75	Precisely dating the Frasnian–Famennian boundary: implications for the cause of the Late Devonian mass extinction. Scientific Reports, 2018, 8, 9578.	1.6	53
76	Late Variscan "Basin and Range―magmatism and tectonics in the Central Alps: evidence from U-Pb geochronology. Geodinamica Acta, 1995, 8, 82-98.	2.2	52
77	Disentangling the Hettangian carbon isotope record: Implications for the aftermath of the endâ€Triassic mass extinction. Geochemistry, Geophysics, Geosystems, 2012, 13, .	1.0	50
78	Late Variscan Magmatic Evolution of the Alpine Basement. , 1993, , 171-201.		49
79	Timing of global regression and microbial bloom linked with the Permian-Triassic boundary mass extinction: implications for driving mechanisms. Scientific Reports, 2017, 7, 43630.	1.6	48
80	The Central Aar Granite: Highly differentiated calc-alkaline magmatism in the Aar Massif (Central Alps,) Tj ETQq0	00 rgBT	/Overlock 107
81	Climate control on banded iron formations linked to orbital eccentricity. Nature Geoscience, 2019, 12, 369-374.	5.4	46
82	The evolution of the polymetamorphic basement in the Central Alps unravelled by precise U?Pb zircon dating. Contributions To Mineralogy and Petrology, 1993, 113, 466-478.	1.2	45
83	Megacrystic zircon with planar fractures in miaskite-type nepheline pegmatites formed at high pressures in the lower crust (Ivrea Zone, southern Alps, Switzerland). American Mineralogist, 2015, 100, 83-94.	0.9	45
84	The isotopic evolution of the Kohistan Ladakh arc from subduction initiation to continent arc collision. Geological Society Special Publication, 2019, 483, 165-182.	0.8	45
85	Rapid eruption of silicic magmas from the Paraná magmatic province (Brazil) did not trigger the Valanginian event. Geology, 2020, 48, 1174-1178.	2.0	45
86	Bracketing the Age of Magmatic-Hydrothermal Activity at the Cerro de Pasco Epithermal Polymetallic Deposit, Central Peru: A U-Pb and 40Ar/39Ar Study. Economic Geology, 2009, 104, 479-504.	1.8	44
87	Thermal erosion of cratonic lithosphere as a potential trigger for mass-extinction. Scientific Reports, 2016, 6, 23168.	1.6	44
88	Geology, Geochronology, and Hf and Pb Isotope Data of the Raul-Condestable Iron Oxide-Copper-Gold Deposit, Central Coast of Peru. Economic Geology, 2006, 101, 281-310.	1.8	43
89	Dating multiply overprinted granites: The effect of protracted magmatism and fluid flow on dating systems (zircon U-Pb: SHRIMP/SIMS, LA-ICP-MS, CA-ID-TIMS; and Rb–Sr, Ar–Ar) – Granites from the Western Erzgebirge (Bohemian Massif, Germany). Chemical Geology, 2019, 519, 11-38.	1.4	41

 $_{90}$  Zircon Uâ  $\in$  "Pb geochronology of Ordovician magmatism in the polycyclic Ruitor Massif (Internal W) Tj ETQq0 0 0 rgBT /Overlock 10 Tf  $_{40}^{50}$ 

#	Article	IF	CITATIONS
91	Model of successive granite sheet emplacement in transtensional setting: Integrated microstructural and anisotropy of magnetic susceptibility study. Tectonics, 2007, 26, .	1.3	40
92	Zircon petrochronology reveals the timescale and mechanism of anatectic magma formation. Earth and Planetary Science Letters, 2018, 495, 213-223.	1.8	40
93	Geochemical Constraints Provided by the Freetown Layered Complex (Sierra Leone) on the Origin of High-Ti Tholeiitic CAMP Magmas. Journal of Petrology, 2017, 58, 1811-1840.	1.1	39
94	Zircon Petrochronology and 40Ar/39Ar Thermochronology of the Adamello Intrusive Suite, N. Italy: Monitoring the Growth and Decay of an Incrementally Assembled Magmatic System. Journal of Petrology, 2019, 60, 701-722.	1.1	38
95	Formation of intra-arc volcanosedimentary basins in the western flank of the central Peruvian Andes during Late Cretaceous oblique subduction: field evidence and constraints from U?Pb ages and Hf isotopes. International Journal of Earth Sciences, 2005, 94, 231-242.	0.9	37
96	Neoproterozoic glaciation in the Proto-Andes: Tectonic implications and global correlation. Geology, 2007, 35, 1095.	2.0	37
97	Contrasting magma types and timing of intrusion in the Permian layered mafic complex of Mont Collon (Western Alps, Valais, Switzerland): evidence from U/Pb zircon and 40Ar/39Ar amphibole dating. Swiss Journal of Geosciences, 2007, 100, 125-135.	0.5	36
98	Kî—ʿAr systematics of clay-to-mica minerals in a multi-stage low-grade metamorphic evolution. Chemical Geology, 1995, 124, 305-316.	1.4	34
99	Dating the Paleoproterozoic snowball Earth glaciations using contemporaneous subglacial hydrothermal systems. Geology, 2017, 45, 667-670.	2.0	33
100	Linking the thermal evolution and emplacement history of an upper-crustal pluton to its lower-crustal roots using zircon geochronology and geochemistry (southern Adamello batholith, N.) Tj ETQq0 0 (	)rgB2∏/Ov	erløzk 10 Tf 5
101	<scp>GZ</scp> 7 and <scp>GZ</scp> 8 – Two Zircon Reference Materials for <scp>SIMS</scp> Uâ€Pb Geochronology. Geostandards and Geoanalytical Research, 2018, 42, 431-457.	1.7	32
102	High-precision U–Pb ages in the early Tithonian to early Berriasian and implications for the numerical age of the Jurassic–Cretaceous boundary. Solid Earth, 2019, 10, 1-14.	1.2	32
103	New high precision U-Pb ages and Hf isotope data from the Karoo large igneous province; implications for pulsed magmatism and early Toarcian environmental perturbations. Results in Geochemistry, 2020, 1, 100005.	0.3	32
104	Long-term repeatability and interlaboratory reproducibility of high-precision ID-TIMS U–Pb geochronology. Journal of Analytical Atomic Spectrometry, 2021, 36, 1466-1477.	1.6	32
105	U-Pb zircon age of volcaniclastic layers in Middle Triassic platform carbonates of the Austroalpine Silvretta nappe (Switzerland). Swiss Journal of Geosciences, 2008, 101, 595-603.	0.5	31
106	Geochronology of a composite granitoid pluton: a high-precision ID-TIMS U–Pb zircon study of the Variscan Karkonosze Granite (SW Poland). International Journal of Earth Sciences, 2014, 103, 683-696.	0.9	31
107	A Hf-isotope perspective on continent formation in the south Peruvian Andes. Geological Society Special Publication, 2015, 389, 305-321.	0.8	31
108	Late Paleozoic to Jurassic chronostratigraphy of coastal southern Peru: Temporal evolution of sedimentation along an active margin. Journal of South American Earth Sciences, 2013, 47, 179-200.	0.6	30

#	Article	IF	CITATIONS
109	The fate of zircon during <scp>UHT</scp> – <scp>UHP</scp> metamorphism: isotopic (U/Pb,) Tj ETQq1 1 0.784	1314 rgBT 1.6	/Qyerlock 1
110	The age of volcanic tuffs from the Upper Freshwater Molasse (North Alpine Foreland Basin) and their possible use for tephrostratigraphic correlations across Europe for the Middle Miocene. International Journal of Earth Sciences, 2018, 107, 387-407.	0.9	29
111	The mafic–ultramafic rock association of Loderio–Biasca (lower Pennine nappes, Ticino, Switzerland): Cambrian oceanic magmatism and its bearing on early Paleozoic paleogeography. Chemical Geology, 2002, 186, 265-279.	1.4	28
112	Experimental evidence for mineral-controlled release of radiogenic Nd, Hf and Pb isotopes from granitic rocks during progressive chemical weathering. Chemical Geology, 2019, 507, 64-84.	1.4	28
113	Early Cambrian oceanic plagiogranite in the Silvretta Nappe, eastern Alps: geochemical, zircon U-Pb and Rb-Sr data from garnet-hornblende-plagioclase gneisses. Geologische Rundschau: Zeitschrift Fur Allgemeine Geologie, 1996, 85, 822-831.	1.3	26
114	Hf isotope analysis of small zircon and baddeleyite grains by conventional Multi Collector-Inductively Coupled Plasma-Mass Spectrometry. Chemical Geology, 2016, 433, 12-23.	1.4	25
115	Zircon petrochronology in large igneous provinces reveals upper crustal contamination processes: new U–Pb ages, Hf and O isotopes, and trace elements from the Central Atlantic magmatic province (CAMP). Contributions To Mineralogy and Petrology, 2021, 176, 1.	1.2	25
116	Stability and isotopic dating of monazite and allanite in partially molten rocks: examples from the Central Alps. Swiss Journal of Geosciences, 2009, 102, 15-29.	0.5	24
117	Heavy rare-earth element enrichment in granites of the Aar Massif (Central Alps, Switzerland). Chemical Geology, 1990, 89, 49-63.	1.4	23
118	Dynamics of the Largest Carbon Isotope Excursion During the Early Triassic Biotic Recovery. Frontiers in Earth Science, 2020, 8, .	0.8	23
119	Estimates of Volume and Magma Input in Crustal Magmatic Systems from Zircon Geochronology: The Effect of Modeling Assumptions and System Variables. Frontiers in Earth Science, 0, 4, .	0.8	21
120	Post-magmatic resetting of Rb-Sr whole rock ages — a study in the Central Aar Granite (Central Alps,) Tj ETQqO	0 0 <sub>1.3</sub> gBT /	Overlock 10
121	Anchoring the Late Devonian mass extinction in absolute time by integrating climatic controls and radio-isotopic dating. Scientific Reports, 2020, 10, 12940.	1.6	19
122	Local melt contamination and global climate impact: Dating the emplacement of Karoo LIP sills into organic-rich shale. Earth and Planetary Science Letters, 2022, 579, 117371.	1.8	19
123	Karst bauxite formation during Miocene Climatic Optimum (central Dalmatia, Croatia): mineralogical, compositional and geochronological perspectives. International Journal of Earth Sciences, 2021, 110, 2899-2922.	0.9	18
124	The ICPMS signal as a Poisson process: a review of basic concepts. Journal of Analytical Atomic Spectrometry, 2015, 30, 1297-1321.	1.6	17
125	High-precision time-space correlation through coupled apatite and zircon tephrochronology: An example from the Permian-Triassic boundary in South China. Geology, 2017, 45, 83-86.	2.0	17
126	Miocene syn-rift evolution of the North Croatian Basin (Carpathian–Pannonian Region): new constraints from Mts. Kalnik and PožeÅįka gora volcaniclastic record with regional implications. International Journal of Earth Sciences, 2020, 109, 2775-2800.	0.9	17

#	Article	IF	CITATIONS
127	Volcanic ash layers in the Upper Cretaceous of the Central Apennines and a numerical age for the early Campanian. International Journal of Earth Sciences, 2004, 93, 384-399.	0.9	15
128	Pluton construction and deformation in the Sveconorwegian crust of SW Norway: Magnetic fabric and U-Pb geochronology of the Kleivan and Sjelset granitic complexes. Precambrian Research, 2018, 305, 247-267.	1.2	14
129	Lifetime of an ocean island volcano feeder zone: constraints from U–Pb dating on coexisting zircon and baddeleyite, and 40Ar/39Ar age determinations, Fuerteventura, Canary IslandsThis article is one of a series of papers published in this Special Issue on the theme of Geochronology in honour of Tom Krogh Canadian lournal of Earth Sciences. 2011. 48. 567-592.	0.6	12
130	The importance of high precision in the evaluation of U-Pb zircon age spectra. Chemical Geology, 2022, 603, 120913.	1.4	12
131	Comment on "A high-precision 40Ar/39Ar age for the Nördlinger Ries impact crater, Germany, and implications for the accurate dating of terrestrial impact events―by Schmieder et al. (Geochimica et) Tj ETQq1 I	0.78431	4 ngBT /Overl
132	10. Petrochronology of Zircon and Baddeleyite in Igneous Rocks: Reconstructing Magmatic Processes at High Temporal Resolution. , 2017, , .		9
133	Timing of K-alkaline magmatism in the Balkan segment of southeast European Variscan edifice: ID-TIMS and LA-ICP-MS study. International Journal of Earth Sciences, 2018, 107, 1175-1192.	0.9	9
134	Constraining Sinistral Shearing in NW Ireland: A Precise U–Pb Zircon Crystallisation Age for the Ox Mountains Granodiorite. Irish Journal of Earth Sciences, 2005, 23, 55-63.	0.3	7
135	Detection in LA-ICPMS: construction and performance evaluation of decision rules. Journal of Analytical Atomic Spectrometry, 2016, 31, 597-630.	1.6	6
136	New age constraints on the palaeoenvironmental evolution of the late Paleozoic back-arc basin along the western Gondwana margin of southern Peru. Journal of South American Earth Sciences, 2018, 82, 165-180.	0.6	6
137	Comment on "Ultrapotassic magmatism in the heyday of the Variscan Orogeny: the story of the TÅ™ebÃÄ• Pluton, the largest durbachitic body in the Bohemian Massif―by JanouÅjek et al International Journal of Earth Sciences, 2021, 110, 1127-1132.	0.9	6
138	The zircon Hf isotope archive of rapidly changing mantle sources in the south Patagonian retro-arc. Bulletin of the Geological Society of America, 2019, 131, 587-608.	1.6	5
139	Reassessing the intrusive tempo and magma genesis of the late Variscan Aar batholith: U–Pb geochronology, trace element and initial Hf isotope composition of zircon. Swiss Journal of Geosciences, 2022, 115, .	0.5	5
140	Response to comment on "Evaluating the temporal link between the Karoo LIP and climatic–biologic events of the Toarcian Stage with high-precision U–Pb geochronology― Earth and Planetary Science Letters, 2016, 434, 353-354.	1.8	4
141	Timing of recovery from the end-Permian extinction: Geochronologic and biostratigraphic constraints from south China: COMMENT AND REPLY: COMMENT. Geology, 2007, 35, e135-e135.	2.0	3
142	The Lithospheric Mantle Beneath Central Europe: Nd Isotopic Constraints for Its Late Proterozoic Enrichment and Implications for Early Crustal Evolution. Geophysical Monograph Series, 2013, , 269-276.	0.1	2
143	Mass Spectrometry in Earth Sciences: The Precise and Accurate Measurement of Time. Chimia, 2014, 68, 124-128.	0.3	2